Analytical and Bioanalytical Chemistry (2023) 415:6711–6721
https://doi.org/10.1007/s00216-023-04948-5

RESEARCH PAPER

Loading characteristics of streptavidin on polypropylene capillary channeled polymer fibers and capture performance towards biotinylated proteins

Md Khalid Bin Islam[1] · **R. Kenneth Marcus**[1]

Received: 20 July 2023 / Revised: 30 August 2023 / Accepted: 11 September 2023 / Published online: 23 September 2023

Abstract

The development of higher-throughput, potentially lower-cost means to isolate proteins, for a variety of end uses, is of continuing emphasis. Polypropylene (PP) capillary-channeled polymer (C-CP) fiber columns are modified with the biotin-binding protein streptavidin (SAV) to capture biotinylated proteins. The loading characteristics of SAV on fiber supports were determined using breakthrough curves and frontal analysis. Based on adsorption data, a 3-min on-column loading at a flow rate of 0.5 mL min^{-1} (295.2 cm h^{-1}) with a SAV feed concentration of 0.5 mg mL^{-1} produces a SAV loading capacity of 1.4 mg g^{-1} fiber. SAV has an incredibly high affinity for the small-molecule biotin (10^{-14} M), such that this binding relationship can be exploited by labeling a target protein with biotin via an Avi-tag. To evaluate the capture of the biotinylated proteins on the modified PP surface, the biotinylated versions of bovine serum albumin (b-BSA) and green fluorescent protein (b-GFP) were utilized as probe species. The loading buffer composition and flow rate were optimized towards protein capture. The non-ionic detergent Tween-20 was added to the deposition solutions to minimize non-specific binding. Values of 0.25–0.50% (v/v) Tween-20 in PBS exhibited better capture efficiency, while minimizing the non-specific binding for b-BSA and b-GFP, respectively. The C-CP fiber platform has the potential to provide a fast and low-cost method to capture targeted proteins for applications including protein purification or pull-down assays.

Keywords Protein purification · Pull-down · Streptavidin · Biotin · Capillary-channeled polymer · Fibers

Introduction

Purification of proteins and antibodies from complex biological samples has grown as a key process in the biotechnology and pharmaceutical industries, offering diverse applications in diagnostics, therapeutics, and fundamental biochemical research [1–3]. A wide range of innovative uses, including recombinant protein therapies, monoclonal antibody-based treatments, and the emergence of personalized medicine, have fueled the development of new separation technologies [4, 5]. The escalating need for proteins and antibodies for diverse applications has catalyzed the expansion of the global chromatography market. As of 2020, the market for chromatography resins has exceeded a value of US $6.0 billion [6]. To address the issues of purifying specific targets, new ligands and resin materials have been introduced to improve separation efficiency. Significant progress has been achieved in the development of affinity-based enrichment methodologies during the past few decades, particularly in the areas of ligand discovery, resin development, and process optimization [7, 8].

Affinity-based purification relies on the specific binding of the target molecule to a ligand immobilized on a solid support. Biotin tagging of target molecules has widespread applications in protein purification, antibody isolation, and bioconjugation techniques [9, 10]. Due to its extremely high affinity for biotin, streptavidin (SAV) is widely used as the capture ligand in the case of biotinylated protein purifications. With a dissociation constant (K_D) of 10^{-14} M, the streptavidin-biotin interaction is considered as one of the strongest non-covalent interactions known, allowing for highly specific and stable binding [11]. Because of the low contributions to further non-specific binding and coincident rapid binding kinetics, the streptavidin-biotin interaction is

✉ R. Kenneth Marcus
marcusr@clemson.edu

[1] Department of Chemistry, Biosystems Research Complex, Clemson University, Clemson, SC 29634-0973, USA

a highly efficient approach for purifying biomolecules. This methodology has been used for a variety of purposes, including target protein purification, proteomics, protein pull-down assays, and the investigation of protein-protein interactions [12, 13]. However, even with such a strong interaction of the streptavidin-biotin complex, non-specific binding can occur, most commonly with the support material, resulting in lower target protein purity and yield [14]. The choice of solid support, thus, has aspects of surface coverage, non-specific binding, mass transfer kinetics, processibility, and ultimately cost.

A crucial step in the effective application of streptavidin-biotin affinity chromatography for the purification of proteins and antibodies is the immobilization of SAV onto a solid substrate. For SAV immobilization, a number of commercially available support phases have been developed over the years. Agarose-, acrylamide-, and sepharose-based support phases have been reported in ligand receptor and cell surface protein capture studies [15, 16]. Agarose, with its large pore size and low non-specific binding, is a popular choice in affinity chromatography. However, agarose support phases have limitations regarding low mechanical stability at high operating pressures in the high-performance liquid chromatography (HPLC) systems [17]. Streptavidin-coated magnetic beads are another viable support phase, allowing rapid initial capture from bulk solution and particle isolation via application of a simple magnetic field [18]. The magnetic beads have an iron oxide layer which can be functionalized with a ligand that binds streptavidin capture ligand. Various streptavidin magnetic bead products have been described for use in proteomic workflows [19–21]. Several benefits of magnetic beads include their high binding capacity and rapid kinetics. Nevertheless, magnetic beads can suffer from aggregation [22], leading to reduced binding efficiency and increased nonspecific binding. Finally, use of streptavidin beads in large-scale protein purification presents a considerable hurdle due to their high cost.

In general, reliable, stable, high-throughput, and cost-effective supports that can deliver high ligand binding capacity and maximum protein capture are needed across the protein purification and diagnostics space. Marcus et al. have demonstrated the use of capillary-channeled polymer (C-CP) fibers as stationary phases for the isolation and purification of proteins [23–25] and of bionanovesicles including exosomes and virus particles [25–27]. C-CP fibers can be extruded from base polymers of nylon-6, polypropylene, and polyester, presenting a range of surface hydrophobicities, ionic character, and functionality. The fiber phases have been employed both in standard HPLC columns and spin-down tip formats [28–30] with the latter allowing for rapid throughput and parallel processing. A number of relatively simple fiber surface modifications have been implemented to affect protein separation selectivity including amination [31], carboxylation [32], and biotinylation [33]. Interactions between macromolecules and the very hydrophobic polypropylene (PP) C-CP fiber surface result in physical adsorption. This phenomenon has led to the application of these fibers as a support phase for the robust immobilization of protein A and achieving immunoglobulin G (IgG)-specific capture both in the column and spin-down tip formats [34–36].

Beyond their chemical characteristics towards affecting separations, C-CP fibers possess a distinct characteristic in the form of eight capillary channels that extend along their length. These capillary channels exhibit interdigitating properties, enabling the formation of well-aligned micrometer-sized channels when the fibers are packed into a column format [23, 37]. This unique shape allows for high volume flow rates (1 mL min^{-1}) with low back pressure (< 250 psi). Very favorable mass transfer rates are possible due to the non-porous surface of the C-CP fibers which facilitates faster protein capture [38, 39]. Moreover, C-CP fibers are fairly inexpensive (~ US \$28 kg^{-1}), whereas a typical microbore column is composed of < 1 g of support material.

In this study, the potential of PP C-CP fibers as support phases for the immobilization of SAV through direct adsorption is explored as a means to capture specific biotinylated target proteins. To achieve this, the C-CP-fiber-packed microbore column format was employed on an HPLC system. Frontal analysis was performed on columns at different ligand concentration levels and volumetric flow rates to determine the dynamic loading characteristics of SAV on the PP C-CP fibers. These results provide the optimal loading conditions for generating the SAV-modified protein capture columns. In the second part of the study, the capture efficiency of biotinylated bovine serum albumin (b-BSA) with a fluorescent tag and a biotinylated green fluorescent protein (b-GFP) was evaluated using the UV-Vis absorbance and fluorescent detectors. Optimization of the protein loading conditions (e.g., flow rate and solvent composition) was undertaken to evaluate the balance between targeted protein capture and minimization of non-specific binding. It is believed that the C-CP fiber surface will evolve as an efficient and cost-effective platform for targeted (biotinylated) protein capture, including preparative column formats, as well as spin-down tips applicable for high-throughput pull-down assays.

Materials and methods

Chemicals and solution preparation

Deionized (DI) water was obtained from a Milli-Q purification system (18.2 MΩ-cm, purified with Millipore, Merck, Germany). Gibco phosphate-buffered solution (PBS) 10× pH 7.4 (ThermoScientific, MA, USA) was diluted in DI

water to prepare 1× solution which was used as a stock PBS for further material dilutions. Bovine serum albumin (BSA) (Sigma-Aldrich, St. Louis, MO) was prepared as a stock solution at a concentration of 2 mg mL^{-1} in PBS. A 1% (v/v) solution of Tween-20 (VWR, Solon, OH, USA) in PBS was prepared as a stock Tween-20 solution. Streptavidin, biotinylated BSA (b-BSA) with a fluorescein fluorescent tag, green fluorescent protein (GFP), and biotinylated GFP (b-GFP) were all obtained from Integrated Micro-Chromatography System (IMCS) (Columbia, SC, USA) in bulk stock solutions of concentrations of 2.8, 3.11, 1.73, and 1.80 mg mL^{-1}, respectively. All further dilutions were prepared in PBS from the stock solutions. HPLC-grade acetonitrile (ACN) (VWR, PA, USA) was used for cleaning and washing columns.

C-CP fiber column construction and instrumentation

The methodology employed for packing C-CP fibers into PEEK microbore (0.76 mm, i.d.) columns has been previously described [28, 35]. A similar method was used here to pack PP C-CP fibers into a 2.4-mm-i.d., 30-cm-long PEEK tubing (Trajan Scientific and Medical, USA), as an extension of the method to a pneumatically actuated pull-down tip is ultimately envisioned. To ensure low solution flow resistance, a total of 2880 PP fibers were pulled through the column. After the fiber-packed columns were prepared, ACN and DI-H_2O were flushed through at a flow rate of 1 mL min^{-1} using the HPLC system. The flushing continued until a stable baseline was achieved as determined by the UV absorbance detector at 216 nm. To assess the packing uniformity of the constructed fiber columns, the interstitial fraction (ε_i) was determined using uracil retention. The calculated interstitial fraction for all the columns was found to be 0.78, with less than 4% variability, which ensured the consistency and packing uniformity of the constructed columns. Once the stability was confirmed, each column was precisely cut into 10-cm lengths with each column containing an average of 0.3582 g of fiber material. The cleaning and chromatographic experiments were performed using a Dionex Ultimate 3000 HPLC system controlled by Chromeleon 7.0 software. The system consisted of an LPG-3400SD pump, a WPS-3000TSL autosampler, a VWD-3400RS UV–vis absorbance detector, and a VWD FLD detector.

Loading process and dynamic binding capacity of SAV column

The methodology to affect a SAV capture column towards biotinylated proteins follows directly from the method originally developed to immobilize protein A onto PP fibers for IgG capture [34–36]. The loading process and dynamic binding capacity (DBC) of SAV on the PP C-CP fiber column were measured by breakthrough curves and frontal analysis. To immobilize SAV onto the PP C-CP fibers, a simple adsorption process was employed, where 0.5 mg mL^{-1} SAV in PBS buffer was passed through the column until a plateau in the absorbance response was reached indicating surface saturation (3 min) as depicted in Fig. 1. As the solution passes over the fiber surfaces, SAV is continuously adsorbed to the surface until the surface sites became saturated, and SAV is no longer retained. At this point, the optical absorbance dramatically increases to a value equal to that of an ambient SAV solution. The DBC_{50} was calculated based on the SAV feed concentration, flow rate, and loading time [38]. The loading time was taken as the time to reach 50% of feed concentration (termed DBC_{50}) based on the measured optical absorbance values at 216 nm. The loading step was followed by a PBS wash step to return the absorbance to the background level. As a confirmation of the load amount, an elution step with 40% (v/v) ACN in PBS was applied to elute-off the retained SAV from the fiber column. If desired, a given PP fiber column could be re-used through the complete process, stripping the fiber surface of the adsorbed SAV as indicated by the return of the absorbance to background levels. Exposure of the PP fibers to such concentrations of ACN is in fact not deleterious to the virtually chemically inert olefinic surface as demonstrated in repeated uses of PP C-CP fiber columns in reversed-phase protein separations [40]. Likewise, this means of elution points to the hydrophobic nature of the streptavidin-PP fiber surface interaction. (Note that the same approach could, in principle, be used to harvest captured proteins from the capture column with the biotin/SAV complex remaining intact.) Frontal analysis was performed at a constant flow rate of 0.5 mL min^{-1} through the 10-cm-long fiber columns at SAV feed concentrations of 0.05, 0.1, 0.3, 0.5, 0.7, 0.9, and 1.0 mg mL^{-1}. Additionally, the effect of volume flow rates on the loading of SAV was evaluated by passing a 0.5 mg mL^{-1} solution at 0.1, 0.3, 0.5, 0.7, 0.9, and 1.0 mL min^{-1},

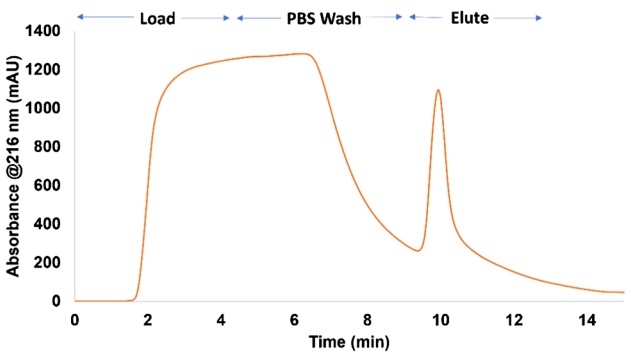

Fig. 1 Response for the load and elution steps of SAV on 10-cm C-CP fiber-packed column. Loading solution: 0.5 mg mL^{-1} SAV, flow rate: 0.5 mL min^{-1}

corresponding to linear velocities of 57.6, 176.4, 295.2, 414, 532.8, and 590.4 cm h^{-1}, respectively.

Binding characteristics of biotinylated proteins on adsorbed SAV

Following the parametric optimization, the SAV-modified column was prepared by loading SAV in a PP-packed 10-cm column at a flow rate of 0.5 mL min^{-1} (295.2 cm h^{-1}) with a 0.5 mg mL^{-1} feed concentration for 3 min. The aim of monitoring protein binding performance on the modified column was to maximize target species capture while minimizing non-specific binding to ensure a selective protein capture strategy. The specific binding of the SAV-modified PP surface was assessed using two biotinylated proteins; biotinylated BSA (b-BSA) with a fluorescence tag and biotinylated GFP (b-GFP). The concept utilized in this system is illustrated in Fig. 2. The integrated elution peak area reflects the unretained biotinylated proteins with the following conditions: no column in-line and SAV-modified column in-line. The fraction of on-column unretained proteins was determined by taking the ratio of the peak area for the pass-through (unretained) species to that obtained without a column. Considering the analytical signal that comes from the total pass through (total unretained species with no column in line) as 100% protein amount injected, the retained amount of the modified column was computed. This parameter, referred to as "capture efficiency" in this study, quantifies the extent to which proteins are retained on the column, normalized to a scale of 100% capture. UV detection at 216 nm was utilized to measure b-BSA capture, and fluorescence excitation at 400 nm and emission at 510 nm were set to measure b-GFP capture. Non-specific binding on the modified surface was assessed from the native BSA and GFP injections. In each case, 4 µg of each of the respective proteins was injected onto the SAV-modified PP fiber column.

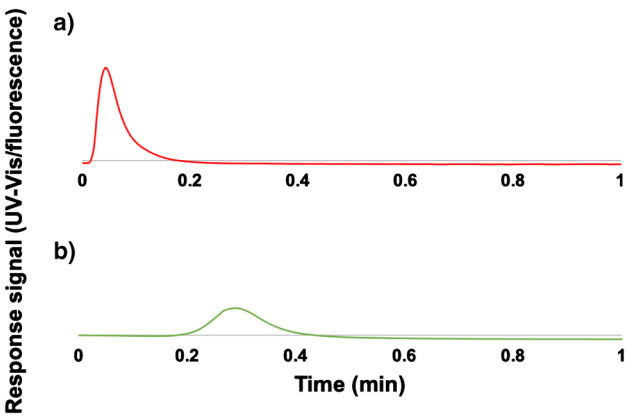

Fig. 2 Typical injection profile of biotinylated proteins with (**a**) no column in-line and (**b**) SAV-modified column in-line

To assess the impact of flow rate on the binding of the b-BSA and b-GFP, the loading solvent buffer of 1× PBS introduced at volume flow rates of 0.3, 0.5, 0.7, and 0.9 mL min^{-1}, or a range of 176.4–590.4 cm h^{-1} (0.49–1.48 mm s^{-1}) in linear velocity. In order to assess and optimize the respective target protein capture while reducing non-specific binding, a systematic investigation of the loading buffer in the presence of the non-ionic detergent Tween-20 was evaluated. Tween-20 concentrations of 0.25%, 0.50%, 0.75%, and 1.0% in PBS (v/v) were explored. Both biotinylated proteins and their native counterparts were injected into the system at a constant loading buffer flow rate of 0.5 mL min^{-1}.

Effects of background proteins

To evaluate the effects of background proteins on the selective capture of the b-GFP, a protein mixture comprising both "soft" and "hard" proteins was prepared. The protein mixture consisted of four proteins with equal mass of ribonuclease A, lysozyme, thyroglobulin, and BSA. By utilizing this protein mixture, the study aimed to assess the impact of background proteins on the selective capture of b-GFP. The inclusion of both "soft" and "hard" proteins in the mixture allowed for a comprehensive evaluation of the binding behavior and selectivity under these conditions. The protein mixture was added to b-GFP to prepare the test separate protein mixture with equal mass ratio of the background and test proteins. A 4-µg protein mixture was injected (20 µL) at a constant flow rate of 0.5 mL min^{-1}. A loading solvent condition of 0.50% (v/v) Tween-20 in PBS was used as it was shown to result in the lowest amount of non-specific binding of GFP.

Results and discussion

SAV loading characteristics

Streptavidin monolayers are commonly used for immobilizing biotinylated proteins, receptors, and DNA due to their strong binding affinity for biotin [41, 42]. In this study, the immobilization of SAV onto the (PP) fibers is investigated through a simple adsorption process. Due to its nonpolar molecular structure, the highly hydrophobic nature of PP fibers dictates that the interaction between SAV and fibers is primarily hydrophobic, as was the case in the protein A and FITC-PEG lipid application [34]. The adsorption of SAV on a hydrophobic surface is typically observed to be irreversible under normal aqueous buffer conditions [43]. The adsorptive ligand loading process here can potentially lead to improper orientation or random geometric orientation of the ligand molecules. Moreover, overloading of the substrate with the SAV capture ligand can lead to steric hindrance that negatively impacts the orientation and accessibility of

binding sites, which in turn can affect the binding affinity and specificity towards the capture molecule. This issue is particularly concerning when working with proteins that possess multiple binding sites. As a result, either the support surface or the neighboring ligands can affect the specificity of the ligand.

To investigate the immobilization of SAV on PP fiber, dynamic binding characteristics were generated from a series of consecutive frontal analysis experiments. These experiments were conducted across a range of SAV input concentrations spanning from 0.05 to 1 mg mL^{-1}. Breakthrough curves were obtained in triplicate at a flow rate of 0.5 mL min^{-1} (295.2 cm h^{-1}). The determined dynamic binding capacities of SAV per mass fiber was plotted (as an adsorption isotherm) as a function of the solute concentration. Figure 3 shows that DBC_{50} values increased in a near-linear fashion with the solute concentration. The dynamic adsorption data was successfully fit to a linear model, yielding a correlation coefficient R^2 of 0.999. Utilizing MATLAB (MathWorks, Natick, MA, USA) software, the data were fit to Langmuir, Freundlich, and BET isotherm models [44]. The Langmuir model exhibited a fit with a correlation coefficient of 0.9945, with the Freundlich and BET models, designed for situations of multilayering or heterogeneous surface adsorption, yielding correlation coefficients of 0.9978 and 0.9984, respectively. Previous investigations have also unveiled similar close-to-linear isotherm trends in diverse adsorption scenarios on C-CP fibers, such as FITC-PEG lipids, staphylococcal protein A on PP fibers, and lysozyme/BSA on PET fibers [35, 45, 46]. It is pertinent to note that protein A adsorption onto PP fibers exhibited a mildly S-shaped isotherm. However, the linear isotherm behavior at lower SAV concentrations aligns well with the isotherm characteristics of FITC-PEG lipid adsorption on PP fibers. Ultimately, the lack of "nonlinear" adsorption phenomena in the responses suggests the absence of surface heterogeneity or multilayering [47]. Given the linear trend of the adsorption isotherm, it is plausible that the maximum capacity of the C-CP fiber column may not have been reached within the employed concentration range (0.05–1 mg mL^{-1} SAV). However, in order to assess the binding capacity of biotinylated proteins on the SAV-modified PP surface, a nominal feed concentration of 0.5 mg mL^{-1} was adopted. This concentration provides a reasonable level of SAV binding on the PP surface, yielding 1.4 mg g^{-1} SAV on the fiber surface (2.7×10^{-8} mol g^{-1} fiber) and well in the range of the linear binding data. Admittedly, this concentration likely represents a compromise in the absolute protein-binding capacity, but sets a good level during these basic studies. Likewise, this implies that there is available fiber surface area wherein non-specific binding might occur.

One other consideration in the on-column loading procedure that can affect the ligand orientation and density is the loading flow rate. Optimization of the flow rate condition can lead to an optimum in mass transfer kinetics for a uniform immobilization on the fiber surface. Figure 4(a) represents the breakthrough curves across the variation of volume flow rates of SAV loading on the C-CP columns. The calculated DBC_{50} values suggest that the mobile phase flow rate has virtually no effect on the SAV adsorption process, yielding dynamic binding capacities ranging from 1.37 to 1.41 mg g^{-1} of fiber, a variability of only 0.87 %RSD across these experiments. The uniformity of the adsorption process is reinforced in Fig. 4(b) where the DBC_{50} values are plotted as a function of the column residence time for different flow

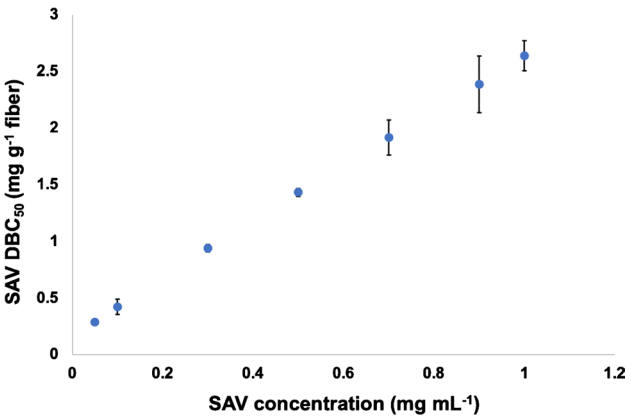

Fig. 3 Dynamic binding capacity (DBC_{50}) of SAV on a PP C-CP fiber column at various feed concentrations

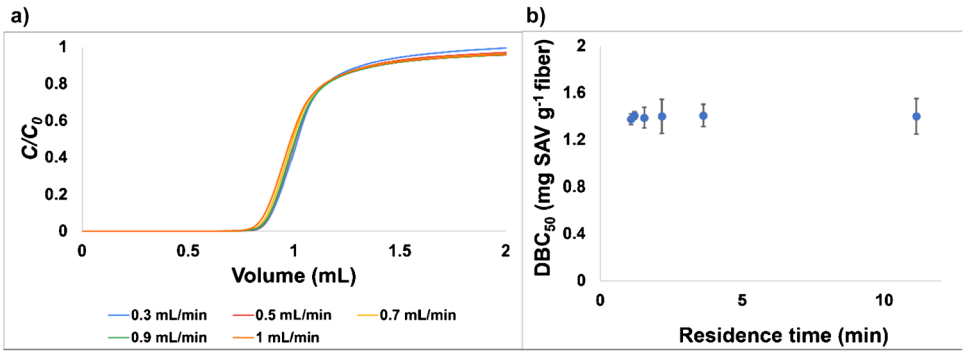

Fig. 4 **a** Breakthrough curves for 0.5 mg mL^{-1} SAV loading on C-CP fiber columns at different flow rates. **b** DBC_{50} plotted as a function of column residence time

rates. The residence time (a function of the void column volume, flow rate, and the column length) can influence the SAV binding to the PP surface. Typically, a longer residence time might suggest greater probabilities for ligand adsorption onto the fiber surface, and indeed greater propensities for multilayering to occur. However, the case is different here for SAV as the DBC_{50} values are found to be virtually identical across the different flow rates. The highest flow rate (1 mL min^{-1}) employed here yields a column residence time of 1.08 min which is sufficient for the column to reach full capacity. Here again, the lower residence times (higher flow rates) show a bit more variability in the data, but certainly acceptable for the pull-down application in general. Since the loading flow rate has minimal effect on SAV loading, a middle range flow rate of 0.5 mL min^{-1} for 3 min was chosen as the SAV loading conditions for further efforts, with a SAV binding capacity of 1.4 mg g^{-1} fiber.

Capture of biotinylated proteins on SAV-modified columns

The primary focus of this effort lies in the overall effectiveness of the SAV immobilized fiber support phase for the successful capture of biotinylated proteins. The quality of any selective protein capture strategy relies on the ability to have maximum target species capture while minimizing the amount of non-specific binding. The binding of biotin to avidin/streptavidin is a rapid and specific process that is recognized as the strongest noncovalent interaction in nature [11]. Despite its effectiveness, non-specific binding to either the ligand or the support can interfere with the desired binding between biotinylated molecule and streptavidin. Therefore, non-specific binding requires careful consideration and evaluation. There is no practical means to bind and elute the affinity-captured proteins due to the strength of the biotin-streptavidin interaction, so that obvious means of assessing binding characteristics (i.e., via the recovery response) is not available. Thus, the process illustrated in Fig. 2 was employed to characterize the fraction of native and biotinylated proteins retained on-column with the former used as a measure of non-specifically bound retention. As will be shown later, the absolute dynamic binding on the column for b-BSA and b-GFP is 131.9 µg and 170.9 µg, respectively. However, in each case, 4 µg of each of the respective proteins was injected onto the SAV-modified PP fiber column which is below the total binding capacity so that variations in the amount of capture can be observed across different conditions (i.e., flow rate, buffer concentrations) without evolind aspects of column overload. The amounts of native BSA and GFP that were retained on the SAV-modified columns were compared to the amount of specifically bound, biotinylated versions of the proteins. The results presented in Fig. 5 demonstrate the capture efficiencies of b-BSA and b-GFP on streptavidin surfaces. It is observed that b-BSA exhibits a capture efficiency of 48.7% (5.4 µg g^{-1} fiber), while b-GFP shows a significantly higher capture efficiency of 98.7% (11.02 µg g^{-1} fiber). From the Avi-tag preparation of the biotinylated proteins, it was assumed that the biotinylation rate was one biotin per GFP molecule, whereas the b-BSA most likely has several biotins per BSA molecule. Therefore, differential capture efficiency is not likely based on the biotinylation process, but rather the higher capture for b-GFP perhaps reflects the smaller globular structure of the protein (MW = 27 kDa) that might experience less steric hindrance with the SAV binding sites in comparison to the b-BSA (MW = 66.5 kDa) [48, 49]. However, the non-specific binding of the native proteins is appreciable with BSA exhibiting a retention of 32% of the injected protein, whereas the native GFP is retained at a level of 20%. These results demonstrate the preferential ability of the target proteins to bind to the SAV-modified PP fiber surfaces while also pointing to appreciable non-specific retention which must be minimized for high-quality purification and pull-down performance.

Effect of flow rate on b-BSA and b-GFP capture

The optimization process of protein adhesion to SAV-modified fiber surface involves a careful balance between thermodynamics and kinetics. Thermodynamics (i.e., surface affinity) energetically drives the proteins to bind to the surface, while kinetics may impose limitations on mass transfer. As

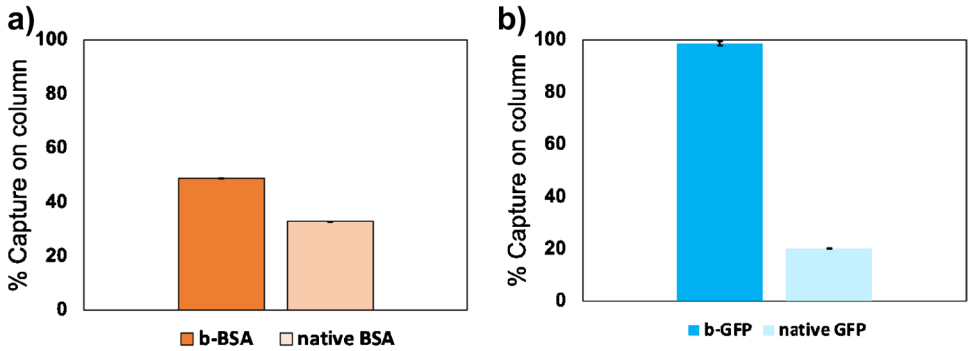

Fig. 5 Capture efficiencies calculated from the recovery of (**a**) b-BSA and BSA injections and (**b**) b-GFP and GFP injections

such, a unique balance may exist in that high-affinity interactions can occur on faster time scales than non-selective ones, meaning that solution flow rate/column residence time can be used to potentially minimize non-specific binding in lieu of the targeted capture. In order to elucidate the potential influence of flow rate on selective capture, we present Fig. 6, illustrating the impact of varying flow rates on the capture efficiency of b-BSA and b-GFP. Mobile phase flow rates ranging from 0.25 to 1 mL min^{-1} were employed. A fourfold increase in solution flow rate does not yield any significant change in the capture efficiency for both b-BSA and b-GFP. This contrasts with previous protein loading experiments conducted on C-CP fibers where increasing the loading flow rate resulted in reduced protein capture [24, 35, 40]. The disparity in findings can be attributed to the distinct hydrodynamics of the analytical column employed in this study which allows longer residence time in comparison to the microbore column used in prior studies (minutes here versus seconds in the previous studies) [35]. Also shown in Fig. 6 are the corresponding retention rates for the native forms of the proteins. In both cases, the biotinylated proteins and native species show little influence regarding flow rates with the percentage of higher retention of the labeled species remaining constant. While no kinetic differences are seen here for specific vs. non-specific binding, experiments discussed in later sections point to definitive kinetic differences when both biotinylated and native species exist in the same solution. Overall, this data holds promise for loading biotinylated proteins with higher flow rates without any decrease in their binding capacity and yield as seen in protein A-IgG studies [34]. Based on these results, a mobile phase flow rate of 0.5 mL min^{-1} was selected for further investigations.

Loading buffer composition

In the context of the selective binding performance of immobilized protein surface, loading buffer composition is crucial in generating high-quality binding data and optimizing performance. Various strategies can be employed to address non-specific interactions including adjustment of buffer pH, incorporation of protein blocking additives, elevation of salt concentration, and introduction of non-ionic surfactants. These approaches have been successfully implemented in diverse experimental methods to control non-specific interactions [50, 51]. Among the options for dealing with non-specific binding caused by hydrophobic interactions, the use of non-ionic surfactants such as Tween-20 is one of the most effective approaches [52]. The addition of small quantities of this mild detergent can effectively interfere with the hydrophobic interactions between the analyte (protein) and the chromatographic surface, thereby mitigating non-specific binding. This strategy holds the potential for reducing undesired interactions and improving the specificity of the binding event. As indicated, Tween-20 functions as a gentle detergent and its influence on the bound SAV on the fiber was not anticipated to result in displacement or degradation. Experiments were conducted to confirm the ligand layer integrity in the presence of Tween-20 prior to the protein capture step, with no appreciable loss in SAV determined. (Further details regarding this experiment can be found in Supplementary Information).

To investigate the impact of mobile phase composition on capture efficiency and non-specific binding, Tween-20 concentrations ranging from 0.25 to 1% in PBS were employed as the mobile phase. As shown in Fig. 7, the capture efficiency of b-BSA increases with the rise in Tween-20 concentration. To be exact, with a fourfold increase in concentration (from 0.25 to 1%), the capture efficiency of b-BSA exhibits an increase of ~ 50%. However, it should be noted that the role of the surfactant on the non-specific capture of native BSA is not straightforward. While not explicitly evaluated, there may be some difference in fluorescence efficiency of the BSA at different concentrations of Tween. While the 0.25% Tween results in the lowest amount of retention, the use of 0.5% perhaps represents the best compromise between selective capture and minimized non-specific binding. In contrast, the capture efficiency of b-GFP remains consistent with the increases in Tween-20 concentration. Here, the non-specific GFP capture also does not follow a straightforward trend, although a notable decrease in non-specific

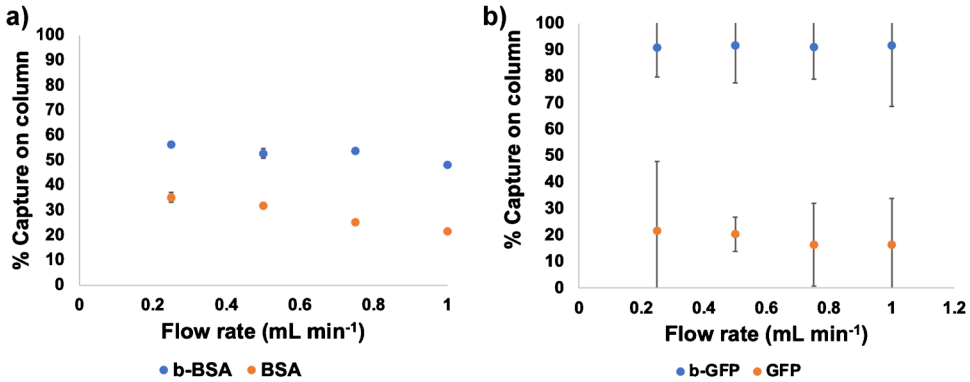

Fig. 6 Capture efficiency calculated from the injection recovery at different flow rates of (**a**) b-BSA and BSA and (**b**) b-GFP and GFP

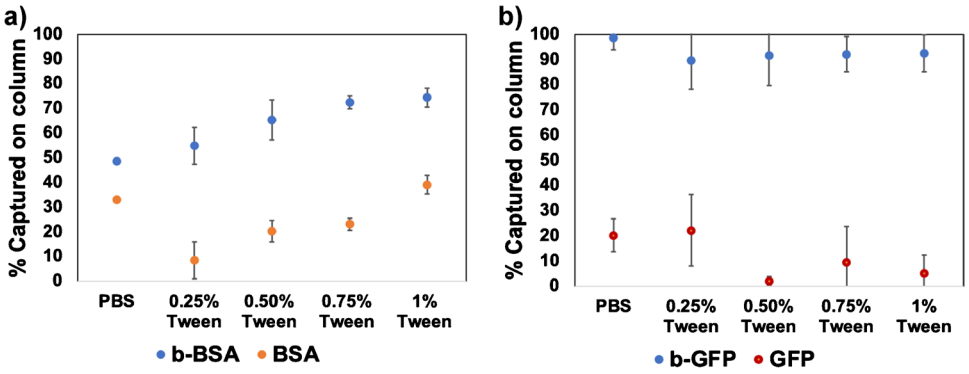

Fig. 7 Effect of Tween-20 concentration on the capture efficiency of (**a**) b-BSA and BSA and (**b**) b-GFP and GFP. Flow rate: 0.5 mL min^{-1}

capture of GFP is observed at 0.5% and 1% Tween-20 in PBS. These findings indicate the varying effects of Tween-20 concentration on the capture efficiency of b-BSA and b-GFP. While b-BSA shows an overall increase in capture efficiency with increasing Tween-20 concentration, b-GFP exhibits a more stable capture performance. It is to be noted that the selective binding performance on the SAV-modified fiber was determined by the amount of biotinylated protein bound to the column in comparison to the protein loaded at the column by-pass position. Exploring its efficacy relative to a non-SAV-loaded column (i.e., unmodified PP fiber) under non-binding conditions could offer valuable insights. Notably, the minimal non-specific binding was observed at the conditions of 0.25% Tween-20 for BSA and 0.50% Tween-20 for GFP, presenting an avenue for assessing selective binding performance. Therefore, biotinylated proteins were injected under these conditions with the SAV column modified and unmodified. The determined protein capture efficiency, comparing the SAV-modified column to the bare PP fiber surface, yielded 55.3% (6.17 μg g^{-1} fiber) for b-BSA and 95.2% (10.63 μg g^{-1} fiber) for b-GFP. These findings establish an excellent alignment with the employed methodology. In general, each specific sample type/matrix would require validation, use of 0.5% Tween-20 in the loading in PBS presents a good compromise in terms of selective capture and minimization of non-specific binding.

Dynamic binding capacity of biotinylated proteins and column-to-column reproducibility

To understand the dynamics of protein adsorption on the SAV-modified PP fiber surfaces, it is critical to analyze the breakthrough curves of the biotinylated proteins. The breakthrough curves of b-BSA and b-GFP on streptavidin-modified PP fiber columns were examined, and the DBC_{50} of each protein was calculated to quantify the maximum amount of protein that can be loaded onto the column. Figure 8 represents the results of the frontal analysis of the breakthrough curves and reveals differences in the DBC_{50} values between b-BSA and b-GFP. The DBC_{50} for b-BSA was determined

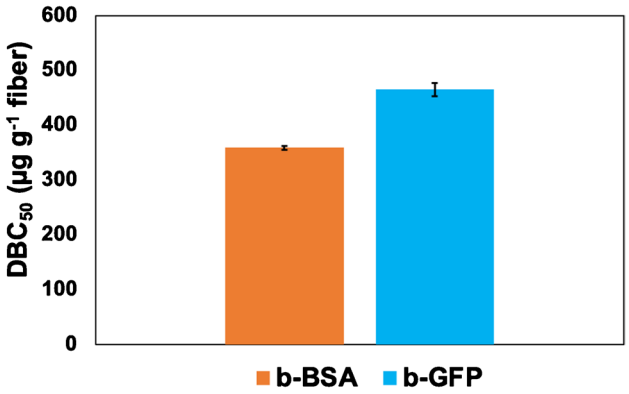

Fig. 8 DBC_{50} of biotinylated proteins on SAV-modified fiber columns

to be 358 μg g^{-1} of fiber while that for b-GFP was found to be higher at 464 μg g^{-1} of fiber. In terms of the number of moles adsorbed on the surface, the amount of b-GFP (1.7×10^{-8} moles g^{-1} fiber) is ~ 3.2 times more than the b-BSA (5.3×10^{-9} moles g^{-1} fiber). The observed discrepancy in molar DBC_{50} values between the two proteins reflects their capture/loading efficiency on the column, with the far greater molecular weight/three-dimensional size (r_{Stokes} 3.48 vs. 2.82 nm) of the BSA molecule limiting the molar coverage and perhaps overall access to the SAV-modified surface. The molar ratio of the DBC values for the captured b-GFP to the SAV surface ligand is 1:1.4, implying a high level of ligand utilization on the C-CP fiber phase. This high level of utilization provides further evidence for the existence of the SAV as a single-layer system.

To assess column-to-column reproducibility of protein binding, three SAV-modified columns were prepared and b-BSA and b-GFP loaded onto the columns at the concentrations, flow rates, and solvent compositions described above. The percentage relative standard deviation (%RSD) value of the protein binding capacity on column was calculated as a measure of the process reproducibility. As presented in Table 1, the reproducibility of the process is outstanding, with the obtained variability for b-BSA and b-GFP binding

of 2.30 and 5.75 %RSD, respectively, reflecting the entirety of the SAV loading process in column formulation as well as the protein capture protocol. This level of performance is outstanding in terms of applications in either protein purification or pull-down applications.

b-GFP capture efficiency in the presence of background proteins

The capture efficiency for a targeted protein can be greatly affected by non-specific binding of competitive background proteins to the surface which reduces the number of available binding sites. Effectively, there are kinetic and thermodynamic factors to consider. As fluorescence could be readily utilized (rather than absorbance) as a means of studying such matrix effects on the b-GFP uptake, the extent of such competition was studied for that case. It was determined that the most favorable binding condition, characterized by reduced non-specific GFP binding, was achieved when using a loading solvent containing 0.5% Tween-20 in PBS (Fig. 9). The performance of b-GFP capture in the presence of background proteins was evaluated using a mixture of proteins, encompassing both "soft" (thyroglobulin and BSA) and "hard" (lysozyme and ribonuclease A) proteins [53, 54]. Figure 9 illustrates the b-GFP capture efficiency in presence of the background proteins. Initially, b-GFP was injected onto the streptavidin-modified fiber column, resulting in a capture efficiency of 91.7% and then with the prepared protein mixture and injected onto the column. Notably, b-GFP still exhibits high capture efficiency with a slight decrease and a capture efficiency of 81% observed in the presence of the protein mixture. These results demonstrate that the protein mixture, consisting of both "soft" and "hard" proteins, has only a modest impact on the selective capture efficiency on the SAV-modified fiber column. As discussed above, there is a competition between the targeted and non-specifically bound proteins, such that the uptake of the labeled protein would impede the non-specific uptake. To ascertain the affinity of the background proteins to the SAV column alone, the protein mixture was injected onto the column without the presence of b-GFP. Here, the background proteins were retained to a level of 58% when no b-GFP was present. This affinity was moderately reduced to 46% in the presence of b-GFP within the mixture. The occurrence of non-specific capture remains notable even in the presence of b-GFP. It

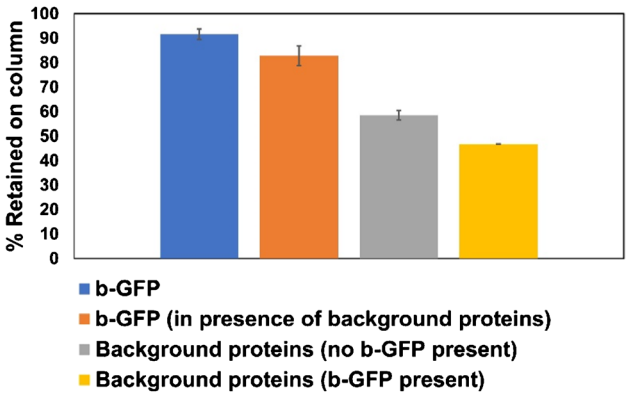

Fig. 9 Effect of background proteins on b-GFP capture. Loading solvent buffer: 0.5% Tween in PBS. Loading flow rate: 0.5 mL min^{-1}

is important to acknowledge that the background protein mixture encompasses a spectrum of both "soft" and "hard" proteins, prone to binding with hydrophobic surfaces. Moreover, any exposed surface area of the PP substrate (under conditions of admitted under-loading) will contribute to non-specific binding. Therefore, the reduction of background protein interaction requires further optimization. However, it proves well that the rapid capture kinetics eventually preclude the uptake of the native proteins in the targeted capture case, while the b-GFP binding performance is not affected significantly in the presence of background protein mixture.

Conclusions

In this work, the polypropylene C-CP fiber surface was investigated as a support phase for SAV immobilization and the eventual capture of biotinylated target proteins. SAV-modified fiber columns were prepared with 3 min on-column loading of SAV on to the bare fiber surface. Optimization of the SAV loading characteristics was performed from the frontal analysis. While higher densities could be readily achieved, a SAV density of 1.4 mg g^{-1} fiber was achieved at a nominal load concentration 0.5 mg g^{-1} and 0.5 mL min^{-1} SAV loading rate. The protein capture efficiency of the modified surface was assessed by injecting two biotinylated proteins: b-BSA and b-GFP. To provide for a more selective binding strategy, with reduced non-specific binding, non-ionic surfactant Tween-20 concentrations in PBS were varied as a loading solvent

Table 1 DBC_{50} for b-BSA and b-GFP on SAV-modified columns and column-to-column variability

	DBC_{50} of b-BSA on SAV-modified column (μg g^{-1} fiber)	%RSD	DBC_{50} of b-GFP on SAV-modified column (μg g^{-1} fiber)	%RSD
Column 1	368.5		477.38	
Column 2	354.5	2.30	488.55	5.75
Column 3	348.96		427.13	

buffer. Studying the effect of flow rate on the loading buffer indicated that the flow rate has minimal effect on either targeted protein capture as well as the non-specific binding. The capture efficiency of b-GFP at optimized loading conditions is not appreciatively affected in the presence of background-interacting protein mixtures. The C-CP platform demonstrates SAV immobilization with relatively high ligand utilization, while further optimization is required to reduce non-specific background protein interaction.

Future efforts will focus on the more practical aspect of capturing biotinylated antibodies from complex media, including protein L on the SAV-modified fiber surfaces. Implementation of the SAV-modified C-CP columns to a tip format allows for implementation in highly automated sample manipulation platforms and coupling to 96-well processing formats. The binding capacities of b-BSA and b-GFP on SAV-modified PP surface is 358 μg g^{-1} (0.291 mg mL^{-1}) and 464 μg g^{-1} (0.386 mg mL^{-1}) fiber, respectively, achieved in a flow through mode in <3 min. Beyond the throughputs realized, per tips costs of <<$1 are very attractive in comparison to commercial phases. The lack of universal reporting standards to compare protein pull-down binding capacities among the different commercial platforms, numerous variable formats of immobilization, and discrepancies in the measurement methods (static vs dynamic) are notable [21]. For example, commercial phases, operated under equilibrium binding conditions over tens of minutes, provide protein capacities of 10× the C-CP fiber tips as applied here. Ultimately, the entire protein capture/elution process, costs, and throughput must be directly compared to the existing commercial processing platforms and materials in order to establish a benchmark for future improvements.

Supplementary Information The online version contains supplementary material available at https://doi.org/10.1007/s00216-023-04948-5.

Acknowledgements We would like to acknowledge Linda Grimes and Dr. Caleb Schlachter at Integrated Micro-Chromatography Systems (IMCS) for helpful discussions and providing the stock solutions of biotinylated BSA (b-BSA) and biotinylated GFP (b-GFP).

Funding This work was financially supported by Integrated Micro-Chromatography Systems (IMCS), Inc. and in part by the US National Science Foundation through grant no. CHE-2107882.

Declarations

Competing interests The authors declare no competing interests.

References

1. Xie W, Wang H, Tong YW, Sankarakumar N, Yin M, Wu D, et al. Specific purification of a single protein from a cell broth mixture using molecularly imprinted membranes for the biopharmaceutical industry. RSC Adv. 2019;9:23425–34.
2. Ghosh R. Ultrahigh-speed, ultrahigh-resolution preparative separation of protein biopharmaceuticals using membrane chromatography. J Sep Sci. 2022;45:2024–33.
3. Kianfar E. Protein nanoparticles in drug delivery: animal protein, plant proteins and protein cages, albumin nanoparticles. J Nanobiotech. 2021;19:159.
4. Garcia CG, Patkar SS, Wang B, Abouomar R, Kiick KL. Recombinant protein-based injectable materials for biomedical applications. Adv Drug Deliv Revs. 2018:114673.
5. Moradi-Kalbolandi S, Hosseinzade A, Salehi M, Merikhian P, Farahmand L. Monoclonal antibody-based therapeutics, targeting the epidermal growth factor receptor family: from herceptin to Pan HER. J Pharm Pharmacol. 2018;70:841–54.
6. Bereli N, Yavuz H, Denizli A. Protein chromatography by molecular imprinted cryogels. J Liq Chromatogr Relat Technol. 2020;43(15–16):657–70.
7. Eifler N, Medaglia G, Anderka O, Laurin L, Hermans P. Development of a novel affinity chromatography resin for platform purification of lambda fabs. Biotechnol Prog. 2014;30(6):1311–8.
8. Arora S, Saxena V, Ayyar BV. Affinity chromatography: a versatile technique for antibody purification. Methods. 2017;116:84–94.
9. de Boer E, Rodriguez P, Bonte E, Krijgsveld J, Katsantoni E, Heck A, et al. Efficient biotinylation and single-step purification of tagged transcription factors in mammalian cells and transgenic mice. Proc Nat Acad Sci. 2003;100(13):7480–5.
10. Aissa AB, Herrera-Chacon A, Pupin R, Sotomayor M, Pividori M. Magnetic molecularly imprinted polymer for the isolation and detection of biotin and biotinylated biomolecules. Biosens Bioelectron. 2017;88:101–8.
11. Green NM. Avidin and Streptavidin in Methods in enzymology, vol 184. Elsevier; 1990. p. 51–67.
12. Kim DI, Roux KJ. Filling the void: proximity-based labeling of proteins in living cells. Trends Cell Biol. 2016;26(11):804–17.
13. Wu KK. Analysis of protein-DNA binding by streptavidin-agarose pulldown. Gene Mapping, Discovery, and Expression: Methods and Protocols. 2006;338:281–90.
14. Luong JH, Male KB, Glennon JD. Biotin interference in immunoassays based on biotin-strept (avidin) chemistry: an emerging threat. Biotechnol Adv. 2019;37(5):634–41.
15 Wollscheid B, Bausch-Fluck D, Henderson C, O'brien R, Bibel M, Schiess R, et al. Mass-spectrometric identification and relative quantification of N-linked cell surface glycoproteins. Nature Biotechnol. 2009;27(4):378–86.
16. Frei AP, Moest H, Novy K, Wollscheid B. Ligand-based receptor identification on living cells and tissues using TRICEPS. Nature Protoc. 2013;8(7):1321–36.
17. Pfaunmiller EL, Paulemond ML, Dupper CM, Hage DS. Affinity monolith chromatography: a review of principles and recent analytical applications. Anal Bioanal Chem. 2013;405:2133–45.
18. Haukanes BI, Kvam C. Application of magnetic beads in bioassays. Bio-Technol. 1993;11:60–3.
19 Filon M, Yang B, Schehr J, Singh A, Bigarella M, Denu J, et al. Abstract B051: Alterations in SIRT2-H3K18Ac identify increased P300 activity in circulating tumor cells from patients with CRPC. Cancer Res. 2023;83(11_Supplement):B051-B.
20. Hussan RH, Dubery IA, Piater LA. Identification of MAMP-responsive plasma membrane-associated proteins in Arabidopsis thaliana following challenge with different LPS chemotypes from Xanthomonas campestris. Pathogens. 2020;9(10):787.
21. Berg-Luecke L, Gundry RL. Assessment of streptavidin bead binding capacity to improve quality of streptavidin-based enrichment studies. J Proteome Res. 2020;20(2):1153–64.
22 Sista RS, Eckhardt AE, Srinivasan V, Pollack MG, Palanki S, Pamula VK. Heterogeneous immunoassays using magnetic beads on a digital microfluidic platform. Lab Chip. 2008;8:2188–96.

23. Nelson DM, Marcus RK. Characterization of capillary-channeled polymer fiber stationary phases for high-performance liquid chromatography protein separations: comparative analysis with a packed-bed column. Anal Chem. 2006;78(24):8462–71.
24. Stanelle RD, Marcus RK. Nylon-6 capillary-channeled polymer (C-CP) fibers as a hydrophobic interaction chromatography stationary phase for the separation of proteins. Anal Bioanal Chem. 2009;393:273–81.
25. Wang L, Marcus RK. Evaluation of protein separations based on hydrophobic interaction chromatography using polyethylene terephthalate capillary-channeled polymer (C-CP) fiber phases. J Chromatogr A. 2019;1585:161–71.
26. Bruce TF, Slonecki TJ, Wang L, Huang S, Powell RR, Marcus RK. Exosome isolation and purification via hydrophobic interaction chromatography using a polyester, capillary-channeled polymer fiber phase. Electrophoresis. 2019;40(4):571–81.
27. Huang S, Bruce TF, Ding H, Wei Y, Marcus RK. Rapid isolation of lentivirus particles from cell culture media via a hydrophobic interaction chromatography method on a polyester, capillary-channeled polymer fiber stationary phase. Anal Bioanal Chem. 2021;413:2985–94.
28. Fornea DS, Wu Y, Marcus RK. Capillary-channeled polymer fibers as a stationary phase for desalting of protein solutions for electrospray ionization mass spectrometry analysis. Anal Chem. 2006;78(15):5617–21.
29. Burdette CQ, Marcus RK. Solid phase extraction of proteins from buffer solutions employing capillary channeled polymer (C-CP) fibers as the stationary phase. Analyst. 2013;138:1098–106.
30. Jackson KK, Powell RR, Bruce TF, Marcus RK. Solid phase extraction of exosomes from diverse matrices via a polyester capillary-channeled polymer (C-CP) fiber stationary phase in a spin-down tip format. Anal Bioanal Chem. 2020;412:4713–24.
31. Jiang L, Jin Y, Marcus RK. Polyethylenimine modified poly(ethylene terephthalate) capillary channeled-polymer (C-CP) fibers for anion exchange chromatography of proteins. J Chromatogr A. 2015;1410:200–9.
32. Jiang L, Marcus RK. Microwave-assisted, grafting polymerization modification of Nylon 6 capillary-channeled polymer fibers for enhanced weak cation exchange protein separations. Anal Chim Acta. 2017;954:129–39.
33. Jiang L, Marcus RK. Biotin functionalized poly(ethylene terephthalate) capillary-channeled polymer fibers as HPLC stationary phase for affinity chromatography. Anal Bioanal Chem. 2015;407:939–51.
34. Schadock-Hewitt AJ, Marcus RK. Initial evaluation of protein A modified capillary-channeled polymer fibers for the capture and recovery of immunoglobulin G. J Sep Sci. 2014;37(5):495–504.
35. Trang HK, Schadock-Hewitt AJ, Jiang L, Marcus RK. Evaluation of loading characteristics and IgG binding performance of Staphylococcal protein A on polypropylene capillary-channeled polymer fibers. J Chromatogr B. 2016;1015:92–104.
36. Trang HK, Marcus RK. Application of protein A-modified capillary-channeled polymer polypropylene fibers to the quantitation of IgG in complex matrices. J Pharm Biomed Anal. 2017;142:49–58.
37. Marcus RK, Davis WC, Knippel BC, LaMotte L, Hill TA, Perahia D, et al. Capillary-channeled polymer fibers as stationary phases in liquid chromatography separations. J Chromatogr A. 2003;986(1):17–31.
38. Randunu KM, Marcus RK. Initial evaluation of protein throughput and yield characteristics on nylon 6 capillary-channeled polymer (C-CP) fiber stationary phases by frontal analysis. Biotechnol Prog. 2013;29(5):1222–9.
39. Randunu JM, Dimartino S, Marcus RK. Dynamic evaluation of polypropylene capillary-channeled fibers as a stationary phase in high performance liquid chromatography. J Sep Sci. 2012;35:3270–80.
40. Randunu KM, Marcus RK. Microbore polypropylene capillary channeled polymer (C-CP) fiber columns for rapid reversed-phase HPLC of proteins. Anal Bioanal Chem. 2012;404:721–9.
41. Raniolo S, Vindigni G, Ottaviani A, Unida V, Iacovelli F, Manetto A, et al. Selective targeting and degradation of doxorubicin-loaded folate-functionalized DNA nanocages. Nanomed Nanotechnol. 2018;14(4):1181–90.
42. Ma M, Zhuang F, Hu X, Wang B, Wen X-Z, Ji J-F, et al. Efficient generation of mice carrying homozygous double-floxp alleles using the Cas9-Avidin/Biotin-donor DNA system. Cell Res. 2017;27(4):578–81.
43. Zareh SK, Wang YM. Single-molecule imaging of protein adsorption mechanisms to surfaces. Microsc Res Techniq. 2011;74(7):682–7.
44. Gritti F, Piatkowski W, Guiochon G. Comparison of the adsorption equilibrium of a few low-molecular mass compounds on a monolithic and a packed column in reversed-phase liquid chromatography. J Chromatogr A. 2002;978:81–107.
45. Schadock-Hewitt AJ, Marcus RK. Loading characteristics and chemical stability of head group-functionalized PEG-lipid ligand tethers on polypropylene capillary-channeled polymer fibers. J Sep Sci. 2014;37:3595–602.
46. Straut CM, Marcus RK. Small molecule adsorption on to polyester capillary-channeled polymer fibers: frontal analysis of naphthalene and naphthol (naphthalene and naphthol adsorption on capillary-channeled polymer fibers). J Sep Sci. 2010;33(1):46–60.
47. Guichon G, Felinger A, Shirazi DG, Katti AM. Fundamentals of Preparative and Nonlinear Chromatography. 2nd Edition ed. Amsterdam: Academic Press. 2006.
48. Demonte D, Dundas CM, Park S. Expression and purification of soluble monomeric streptavidin in Escherichia coli. Appl Microbiol Biot. 2014;98:6285–95.
49. Pavoor TV, Cho YK, Shusta EV. Development of GFP-based biosensors possessing the binding properties of antibodies. Proc Nat Acad Sci. 2009;106(29):11895–900.
50. Désormeaux A, Blochet J-E, Pézolet M, Marion D. Amino acid sequence of a non-specific wheat phospholipid transfer protein and its conformation as revealed by infrared and Raman spectroscopy. Role of disulfide bridges and phospholipids in the stabilization of the α-helix structure. BBA-Protein Struct M. 1992;1121(1–2):137–52.
51. Situ C, Wylie AR, Douglas A, Elliott CT. Reduction of severe bovine serum associated matrix effects on carboxymethylated dextran coated biosensor surfaces. Talanta. 2008;76(4):832–6.
52. Kenna J, Major G, Williams R. Methods for reducing non-specific antibody binding in enzyme-linked immunosorbent assays. J Immunol Methods. 1985;85(2):409–19.
53. Norde W, Lyklema J. Interfacial behaviour of proteins, with special reference to immunoglobulins. A physicochemical study. Adv Colloid Interfac. 2012;179:5–13.
54. Benavidez TE, Torrente D, Marucho M, Garcia CD. Adsorption of soft and hard proteins onto OTCEs under the influence of an external electric field. Langmuir. 2015;31(8):2455–62.